

Uncovering the role of the light-induced reduction of the inter-atomic exchange in the ultrafast demagnetization of Fe, Co, and Ni

Philippe Scheid,^{1,2,3,*} Julius Hohlfeld,³ Gregory Malinowski,³ Anders Bergman,¹ Olle Eriksson,^{1,4} Sébastien Lebègue,² and Stéphane Mangin³

¹*Department of Physics and Astronomy, Uppsala University, Box 516, SE-75120 Uppsala, Sweden*

²*Université de Lorraine, LPCT, CNRS, UMR 7019, BP 70239, 54506 Vandoeuvre-lès-Nancy Cedex, France*

³*Université de Lorraine, IJL, CNRS, UMR 7198, BP 70239, 54000 Nancy Cedex, France*

⁴*School of Science and Technology, Örebro University, SE-701 82, Örebro, Sweden*

(Dated: January 4, 2023)

Time resolved measurements of the linear magneto-optical Kerr rotation reveal that, in the 3d ferromagnets Fe, Co and Ni, the amplitude of the demagnetization increases linearly with the fluence of the light. We rationalize this phenomenon as being linearly driven by the increase in temperature, the electron-phonon and electron-magnon scattering, and a reduction of the inter-atomic exchange. The amplitude of the latter phenomenon, which until the present study has been widely overlooked, is obtained through *ab initio* density functional theory calculations, and is argued to be the principal source of demagnetization in Ni and Co, while still contributing largely in Fe.

More than twenty years ago, Beaupaire *et al.*[1] produced the first experimental evidence of the ultrafast quenching of the magnetic order by femtosecond light pulses. This discovery, and the perspective it held to allow for the manipulation of magnetization in unprecedented timescale, and without the use of a magnetic field, triggered an intense and very fruitful research that is still ongoing. Notably, a few years later, the all-optical switching, in which femtosecond light pulses allow for the deterministic manipulation of the magnetic state of metallic thin films was evidenced[2, 3]. Since then, both the single pulse, all-optical helicity-independent switching, as well as its helicity-dependent counterpart were found in evermore complex structures and compounds[4, 5]. However, regardless of the apparent intricacy of these light-induced studies of magnetisation dynamics, the common denominator of all these phenomena is the presence of an initial ultrafast demagnetization.

Naggingly, up to this day, the inner workings of this overarching phenomenon remain heavily debated, as much from the standpoint of the magnetic excitations responsible for the quenching, as regarding the types of mechanisms by which they are triggered. Early photoemission results[6–9], pointed toward a reduction of the exchange splitting, suggesting induced Stoner excitations, thus inducing a longitudinal decrease of the atomic magnetic moments[10]. More recently Turgut *et al.*[11] and Eich *et al.*[12] explicitly addressed this issue and experimentally showed a predominance of band mirroring in Co, a consequence of the presence of transversal excitations. As opposed to a decrease of the magnitude of each individual atomic magnetic moment, the demagnetization would therefore mainly result from a randomization of their direction. A similar conclusion

has been drawn for bcc Fe[13].

To rationalize such dynamics, many theories have been proposed throughout the years. As reviewed by Scheid *et al.*[10], possible sources of longitudinal excitations have been proposed; such as Elliot–Yafet electron-phonon spin-flip scatterings[14], a spin-dependent superdiffusive propagation of the hot-electrons[15], a light-induced increase of the electronic temperature[16], and a direct light-matter interaction.[17–19] However, these theories were not able to explain the magnitude of the experimentally seen demagnetization, at least within the confinement of the experimentally absorbed energy. On the other hand, ever since the pioneering work of Beaupaire *et al.*[1], various temperature models have been a mean of understanding the characteristics of the demagnetization through a rapid increase of the temperature experienced by the magnetic moments[20–23]. While such a framework does not explain how the angular momentum is conserved during the demagnetization, it provides the most straightforward rationalization of the latter, as originating from an ultrafast heating. Accordingly, in this regime, the demagnetization would occur through the generation of transversal excitations, or magnons, as they are the primary magnetic excitations responsible for the ferromagnetic-paramagnetic phase transition occurring at the Curie temperature in the elements studied here (e.g. as pointed out by Gunnarsson[24]).

In the present, combined experimental and theoretical work, we demonstrate that the maximal demagnetization amplitude in the elemental ferromagnets Fe, Co and Ni challenges the aforementioned heating hypothesis. Indeed, it is argued here that only accounting for purely thermal effects occurring on top of electron-phonon and electron-magnon couplings hardly allows to simultaneously explain the experimentally seen demagnetization

* philippe.scheid@univ-lorraine.fr

amplitude across the compounds. However, utilizing *ab initio* calculations, we provide significant evidences that considering the light-induced reduction of the inter-atomic exchange can rationalize the experimental demagnetization. Hence, rather than driving the magnetic system toward the Curie temperature, T_C , through heating as explained within the three temperature model based on rigid spins, T_C is suggested here to be transiently decreased.

The magnetic films studied here are made of 12 nm of bcc Fe, fcc Co and fcc Ni, all of which are capped by 2 nm of Pt and deposited on a buffer layer of 2 nm of Ta sitting on a glass substrate. The thickness of the films is large enough such that bulk properties are recovered, while the effect of absorption gradients are mitigated by the rapid spreading of hot electrons. The dynamics were probed using a magneto-optical microscope that monitors the longitudinal Kerr effect for spatially uniform s-polarized probe pulses having a wavelength of 515 nm and a duration of 150 fs as function of pump-probe delay. The latter were incident on the samples at an angle of 45° . The normally incident, linearly polarized 800 nm, 150 fs pump pulses were focused on the sample to a $95 \mu\text{m}$ (FWHM) Gaussian. The pump was aligned to the center of the $560 \times 360 \mu\text{m}$ area of the sample displayed on the camera. The spatial resolution of the image was $\approx 10 \mu\text{m}$. In-plane magnetic saturation fields were applied during the measurements to ensure full restoration of the magnetization between the pump-probe pulse pairs. The pulse repetition rate was 50 kHz and the exposure time of the camera was of the order of 1s, so that each image represents the average signal resulting from 50 000 laser pulses. The fluence dependence of the pump induced magnetization dynamics is derived from the measured images in three steps: First, potential artifacts (e.g. from pump induced changes of the non-magnetic sample reflectivity) are suppressed by subtracting the images measured for opposite magnetization directions at identical pump-probe delay, and dividing this difference by the one obtained at negative delay. Second, the spatial variations of the measured magnetization changes are mapped to the ones of the pump beam. Third, external fluences are converted to absorbed ones by means of the TMM python package and the complex indices extracted from Ref.[25].

Fig. 1 a) presents the magnetization dynamics for all three samples for different values of the absorbed fluence. Even though, as expected, all the dynamics are characterized by a very swift reduction of the magnetization, these results challenge the existing viewpoints on multiple accounts.

To further investigate these experimental results, in Fig. 1 b), we consider the maximum relative demagnetization, $m_{\min} = \frac{M_{\min}}{M_0}$, where M_0 and M_{\min} respectively are the magnetization at saturation and the minimum magnetization reached during the dynamics. Doing so shows that the amplitude of the demagnetization increases linearly with the absorbed energy, *i.e.* can be written as:

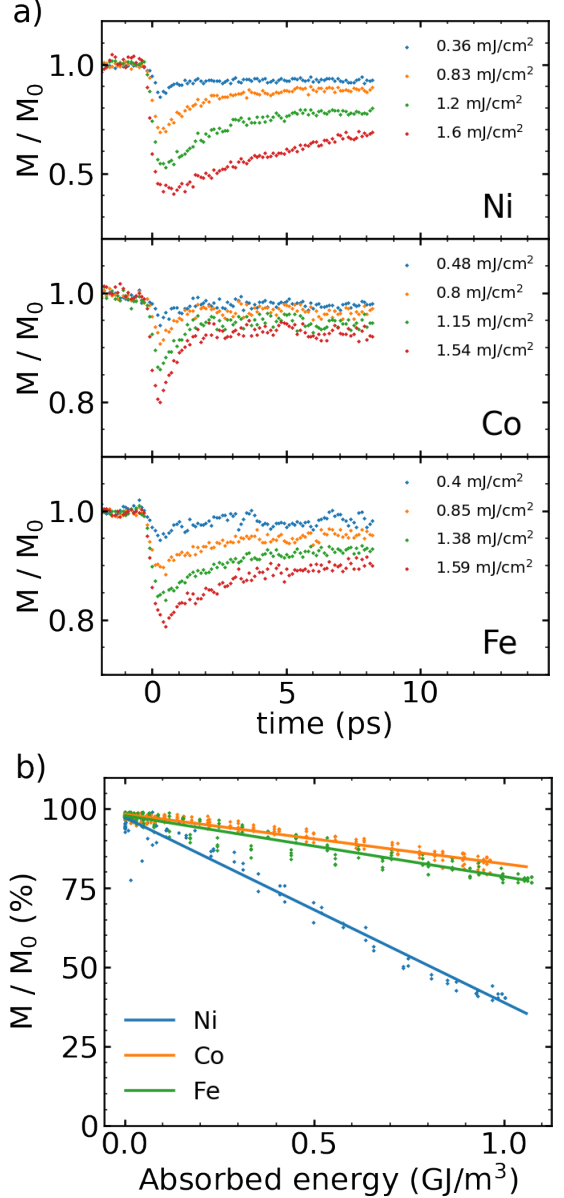


FIG. 1: a) Light-induced ultrafast demagnetization dynamics in Fe, Co and Ni at different absorbed fluences measured using the TR-MOKE. b) Normalized maximum demagnetization, $m_{\min} = \frac{M_{\min}}{M_0}$ as a function of the fluence.

$$m_{\min} = 1 + \alpha_{\text{exp}} E_{\text{abs}} \quad (1)$$

where α_{exp} is the slope, which value is displayed in Tab.I for the different compounds and E_{abs} is the absorbed energy density, computed by dividing the absorbed fluences by the thicknesses of the absorbing films (16 nm).

Interestingly, this linear decrease of the magnetization with the absorbed energy contradicts the well established Bloch law stating that, upon thermal excitation, the

variation of the magnetization is proportional to $T_m^{3/2}$, or equivalently $\propto E_m^{3/5}$ since $E_m \propto T_m^{5/2}$, where T_m and E_m respectively are the temperature and the energy of the magnons.

Nonetheless, as suggested by the fact that it holds the lowest T_C (627 K) of the three compounds studied here, Ni is by far the most easily demagnetized element. On the other hand, and quite surprisingly such a reasoning fails when comparing Co, which has a T_C of 1388 K, with Fe, that has a significantly lower T_C of 1043 K, as both of them present very similar demagnetization amplitudes.

In the framework of temperature models, this unexpected similarity in the value of α_{exp} for Co and Fe, could be the consequence of a larger electron-phonon coupling in Fe than in Co, thus more rapidly evacuating the absorbed energy from its electronic and spin degrees of freedom, and mitigating its demagnetization. Along this line of argument, the very pronounced demagnetization of Ni could originate from a very low electron-phonon coupling that would allow for the light-absorbed energy to almost solely affect the spin system and thus enhance the demagnetization. However, as can be seen in Tab. I recapitulating *ab initio* calculated values from Ritzmann *et al.*[26], the electron-phonon coupling in Fe is more than three times weaker than it is in Co, while in Ni it is located in between, thus invalidating the aforementioned scenario.

Likewise, in a framework where the demagnetization is mostly due to transversal excitations, which, as discussed *supra*, appears to be the case, a high electron-magnon coupling in Ni and Co as compared to Fe could explain the higher demagnetization in Ni and Co and the surprising resilience of Fe. However, as reported in Tab. I, *ab initio* calculations from Haag *et al.*[27] in Fe and Ni show that the electron-magnon scattering rate in Ni is one order of magnitude lower than in Fe. While Haag *et al.*[27] did not treat the case of Co, the work of Müller *et al.*[28] indicates that it is similar to the one in Ni. Indeed, Müller *et al.* reported *ab initio* calculations of the electronic lifetime broadening and band renormalization in Fe, Co and Ni as a consequence of the electron-magnon coupling and found the strongest signatures of the latter in Fe, followed by Co and Ni. Consequently the electron-magnon coupling alone cannot explain the very large demagnetization in Ni and the resilience of Fe either.

One should also note that the demagnetization dynamics in Fe dramatically differs from the one of Co and Ni as, even at low demagnetization amplitudes, it does not feature the so-called quick recovery[9], otherwise present in Ni and particularly in Co. According to You *et al.*[9] the passage from a quick recovery to a slow recovery regime is due to a transient crossing of T_C , however the result presented here contradicts this hypothesis. Indeed, Ni, which has a much lower T_C than Fe, recovers more quickly than Fe, while demagnetizing much more than the latter. Likewise, in the framework

	Ni	Co	Fe
Curie temperature (K)	627	1388	1043
G_{ep} ($10^{17} \text{W}/(\text{m}^3 \text{K})$)	18.9	33.4	10.5
$W_{\text{magnon}}^{\uparrow\downarrow}$ (scattering / 100 fs)	0.15	≈ 0.15	1.34
$\frac{dI}{dE}$ (% $\text{GJ}^{-1} \text{m}^3$)	-48.40	-15.82	-7.85
α_{exp} (% $\text{GJ}^{-1} \text{m}^3$)	-58.51	-15.71	-19.27

TABLE I: Table summarizing the Curie temperature, T_C , and the electron-phonon scattering rates, G_{ep} , from Ref. [26] and electrons-magnons scattering between two dominant spin states per 100 fs and per atom, $W_{\text{magnon}}^{\uparrow\downarrow}$ calculated at an electronic temperature of 900 K in Ref. [27] for Ni and Fe. As discussed in the text, based on Ref. [28] we assessed the value of $W_{\text{magnon}}^{\uparrow\downarrow}$ in Co to be close to the one in Ni. In addition, both the slope of the *ab initio* calculated inter-atomic exchange reduction, as well as the maximum demagnetization experimentally measured as a function as the absorbed energy are recapitulated.

of the microscopic three temperature model[20, 21], the demagnetization rate is governed by the Elliot-Yaffet spin-flip scattering rate and, if the electron-phonon coupling is low enough such that the electronic temperature stays high long enough, the initial demagnetization is followed by a remagnetization. Consequently, in this framework too, Fe, which has the lowest electron-phonon coupling and the largest Elliot-Yaffet spin-flip scattering rate of the three compounds studied here[14], should be more prone to feature a large demagnetization followed by a remagnetization.

To sort out the apparent inconsistencies discussed above, we investigate the involvement of a previously overlooked phenomenon, which we find to be strongly correlated to the magnitude of the demagnetization: the ultrafast light-induced quenching of the inter-atomic exchange. We use *ab initio* density functional theory calculations to compute the dependence of the inter-atomic exchange on the light-absorbed energy. As in our previous work[16], as well as in the framework of the temperature models, the increased electronic energy is accounted for as a rise of the electronic temperature, T_e , such that the occupation of the different Kohn-Sham states obey the Fermi-Dirac distribution. In this framework, the T_e -dependent magnons are obtained within a formalism consisting in a mapping of the energy obtained from density functional theory spin-spiral calculations on the Heisenberg Hamiltonian[29–31]. In the latter, the energy of interaction of an atom indexed by i with all of the other atoms indexed by j writes as:

$$\hat{H}_i(t) = -\frac{1}{2} \sum_{i \neq j} J_{ij} \hat{\mathbf{M}}_j(t) \cdot \hat{\mathbf{M}}_i(t). \quad (2)$$

Neglecting the spin correlations and in the adiabatic approximation, one retrieves the dampingless Landau-

Lifshitz equation for the motion of the atomic magnetic moments[30] $\frac{d\langle \hat{\mathbf{M}}_i \rangle(t)}{dt} \approx -\frac{g\mu_B}{\hbar} \sum_{i \neq j} J_{ij} \langle \hat{\mathbf{M}}_i \rangle(t) \times \langle \hat{\mathbf{M}}_j \rangle(t)$, which eigenstates in crystal lattices, are collective excitations called magnons. When the latter only contains one atom per Bravais lattice point, as it is the case of this work considering bcc-Fe, fcc-Co and fcc-Ni, the magnon states are fully indexed by their wavevector, \mathbf{q} , and their eigenenergies simply write as:

$$\omega_{\mathbf{q}} = \frac{Mg\mu_B}{\hbar} \tilde{J}_{\mathbf{q}}, \quad (3)$$

where $\tilde{J}_{\mathbf{q}} = J_{\mathbf{q}} - J_{\mathbf{q}=0}$, M is the atomic magnetic moment and $J_{\mathbf{q}}$ is the Fourier transform of the real-space Heisenberg exchange J_{ij} :

$$J_{\mathbf{q}} = - \sum_j (1 - \delta_{ij}) J_{ij} e^{i\mathbf{q}(\mathbf{R}_j - \mathbf{R}_i)}. \quad (4)$$

$\tilde{J}_{\mathbf{q}}$ can readily be assessed in density functional theory calculations using the spin-spiral *ansatz*[32], as it relates to the energy, $E_{\mathbf{q}}$ of such a state through:

$$E_{\mathbf{q}} = \frac{1}{2} M^2 \left(J^0 + \tilde{J}_{\mathbf{q}} \sin^2 \theta \right), \quad (5)$$

where E_0 is the electronic energy of the ferromagnetic state, $E_{\mathbf{q}}$ is the electronic energy when the atomic magnetic moments are forming a spin-spiral of wavevector \mathbf{q} and are tilted away from the parallel, ferromagnetic axis by θ .

Finally, in order to obtain the exchange interaction between pairs of atoms indexed by i and j , we performed the inverse Fourier transform of $\tilde{J}_{\mathbf{q}}$, writing as:

$$J_{ij} = -\frac{1}{\Omega_{BZ}} \int_{BZ} d\mathbf{q} e^{-i\mathbf{q}(\mathbf{R}_i - \mathbf{R}_j)} \tilde{J}_{\mathbf{q}} \quad (6)$$

Ground state energies were obtained from density functional theory calculations[33, 34] using the non-collinear full potential augmented plane-wave method (APW) and the LSDA[35] for the exchange correlation potential, as implemented in the ELK code. The APW basis is expanded in 10 spherical harmonics, $|k + G|_{max} R = 8$, where R is the radius of the muffin-tin, and the Brillouin zone is sampled with a 28x28x28 mesh for all the compounds. A large grid is particularly important in order to insure the convergence at low T_e . The self-consistence is achieved when the total energy changes by less than 10^{-8} Ha in two successive electronic loops. The integrals over the first Brillouin zone required in the computation of the density of states (DOS) of the magnons, as well as the real-space inter-atomic exchanges are performed on a $14 \times 14 \times 14$ q-point sampling grid. The DOS are obtained by using a Gaussian smearing of 0.02 eV to replace

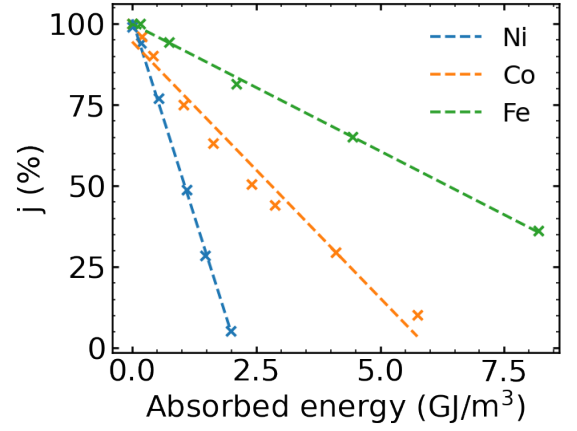


FIG. 2: Normalized inter-atomic exchange in Ni, Co and Fe, as a function of the electronic energy density obtained through *ab initio* spin-spiral calculations.

the Dirac deltas. All of these tasks are performed in a separate, home-made, python code.

We then used this framework to assess the impact of the light on the inter-atomic exchanges within bcc Fe, fcc Co and fcc Ni by computing the latter at different values of the electronic temperature, T_e , and thus of the electronic energy, $E(T_e)$. As in these compounds, long range exchange interactions significantly contribute to the magnetic ordering[31, 36], we computed the effective value of the inter-atomic exchange, j , felt by an atomic site labeled by α , by including all the interactions $J_{\alpha i}(E)$, comprised from the first, up to its 20th neighbors as a function of $E(T_e)$:

$$j(E) = \frac{\sum_i J_{\alpha i}(E)}{\sum_i J_{\alpha i}(E(T_e = 300K))} \quad (7)$$

where the electronic energy, E_e , is readily extracted from the T_e dependent *ab initio* calculations. Note that, as we are only interested in the rate of reduction of the inter-atomic exchange and not in its absolute value, in Eq. 7, we normalized by the same quantity computed at $T_e = 300K$.

Fig. 2, featuring $j(E)$, shows that the inter-atomic exchange decreases linearly with the increased electronic energy. Quite remarkably, this reduction is far from being negligible in the range of the experimental fluences. This fact is better seen in Tab. I, gathering the slopes of both the maximum demagnetization as a function of the absorbed energy density, shown in Fig. 1 b), and the slope of the decrease of j as a function of the absorbed energy shown in Fig. 2. Strikingly, in Ni and Co both rates of decrease are matching quite closely, while in Fe the rate of the decrease of the exchange is half the one of the maximum demagnetization. This apparent correlation between the maximum demagnetization and the *ab initio* calculated reduction of the exchange points toward a novel mechanism where, instead of, or on top of being

the consequence of an increase of the temperature, the demagnetization could be due to a quenching of interaction responsible for the magnetic ordering itself. Indeed, upon reduction of the inter-atomic exchange, the ferromagnetic ordering is expected to decrease through the creation of magnons. While the rate at which magnons are generated may be tied to the damping, the reduction of the inter-atomic exchange is due to its parametric dependence on the electronic state and thus occurs instantaneously with the perturbation brought by the light-pulse. Such a phenomenology is in direct contrast with a transfer of heat from the electrons to the magnons as assumed by temperature models.

Finally, we propose to investigate correlations existing between temperature effects, the reduction of the inter-atomic exchange, the electron-phonon coupling (G_{ep}) and the electron-magnon coupling (G_{em}) in the experimental amplitude of demagnetization (slope of the curves in Fig. 1 b)). To this end, we assume that, as the maximum demagnetization scales linearly with the absorbed energy, it may scale linearly with the amplitude of the four aforementioned phenomena. Assuming that the amplitude of thermal effects scales as the inverse of T_C , we get:

$$\alpha_{\text{fit}}^C(x_T, x_j, x_{G_{ep}}, x_{G_{em}}) = x_T \frac{1}{T_C^C} + x_j \frac{dj^C}{dE} + x_{G_{ep}} G_{ep}^C + x_{G_{em}} G_{em}^C, \quad (8)$$

where x_T , x_j , $x_{G_{ep}}$ and $x_{G_{em}}$ are the fitting coefficients and α_{fit}^C is the fitted slope for the different compounds indexed by C.

Fig. 3 shows α_{fit}^C (purple bar) as well as the different contributions to it (blue, orange, red and green), for Fe, Co and Ni. The figure also shows α_{exp}^C (brown) for all elements investigated here. As the system of equations is under-determined, *i.e.* there are four variables, $\mathbf{x} = (x_T, x_j, x_{G_{ep}}, x_{G_{em}})^T$, and only three constraints given by the experimental slopes of three elements, we look for the solution minimizing $\|\mathbf{x}\|$. Doing so provides the simplest explanation of the experimental slopes. Interestingly, as shown in Fig. 3, such an analysis completely excludes a contribution originating from a rise of the temperature as the explanation for the amplitude of the demagnetization and, instead, attributes it mainly to the quenching of the inter-atomic exchange in Ni and Co. On the other hand, in Fe, and in agreement with the work of Carpenne *et al.*[37], the electron-magnon scattering explains more than half of the demagnetization, while the reduction of the inter-atomic exchange explains the remaining contribution. Supposing that the “quick recovery” regime is, in fact, due to a recovery of the inter-atomic exchange, this may explain why Fe does not feature this phenomenon as strongly as Ni and Co do. Here we also notice that the model correctly attributes a positive sign to $x_{G_{ep}}$, which is in accordance with the aforementioned physical insight that the electron-phonon coupling reduces the amplitude of the maximum demag-

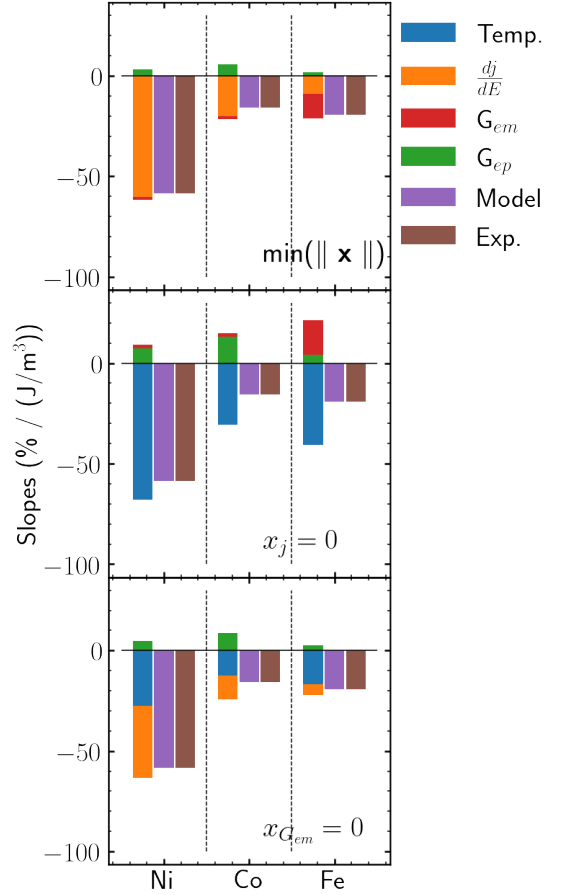


FIG. 3: Contribution to the demagnetization of: (1) thermal fluctuation, $x_T \frac{1}{T_C^C}$, in blue (2) reduction of j as a function of the absorbed energy, $x_j \frac{dj^C}{dE}$, in orange (3) electron-phonon, $x_{G_{ep}} G_{ep}^C$, in green and (4) electron-magnon coupling, $x_{G_{em}} G_{em}^C$, in red to α_{fit}^C , the fitted slope of the maximum demagnetization in purple for Ni, Co and Fe. α_{fit}^C is computed in three different cases: (Top) minimizing the norm of $\mathbf{x} = (x_T, x_j, x_{G_{ep}}, x_{G_{em}})^T$, (Middle) setting $x_j = 0$, (Bottom) setting $x_{G_{em}} = 0$. For comparison the value of the experimental slope, α_{exp}^C is displayed in brown.

netization.

The case when x_j is imposed to be zero is also considered here, *i.e.* placing ourselves in the usual framework in which the reduction of exchange is neglected. In its absence, the model provides inconsistent results: the contribution of the electron-magnon scattering is positive, *i.e.* tends to limit the amplitude of the demagnetization. This emphasizes the necessity of accounting for the involvement of the reduction of the inter-atomic exchange in the demagnetization. Lastly, to provide a range in which this model correctly predicts that $x_{G_{em}} > 0$, we now impose $x_{G_{em}} = 0$. In such a case the temperature has to play a significant role in the explanation of the experimental slopes, and now amounts

for more than a third of the amplitude in Ni and Co and almost entirely takes over in Fe. We expect the physical reality to be located in between the graph on the top, minimizing $\|\mathbf{x}\|$, and this case, *i.e.* $x_{G_{em}} = 0$. That would mean that both the electron-magnon scattering and a rise of the temperature play a role in regulating the amplitude of the demagnetization. However, this model really emphasize that in any case, the reduction of the inter-atomic exchange plays a major role in the explanation of the experimental demagnetization amplitude and cannot be overlooked.

To summarize, the reduction of the inter atomic exchange provides a novel mechanism through which transversal excitations, or magnons can be generated on the ultrafast timescales. Indeed, assuming that some notion of temperature could be defined at such short timescales, rather than simply getting closer to T_C , the initial part of the demagnetization can, in a significant part, be due to a transient reduction of T_C itself, as shown by the linear relation between T_C and the first-neighbors inter-atomic exchange in classical atomistic spin models[30, 38]. As this phenomenon is particularly

strong in Ni, this could notably explain the critical behavior occurring within 20 fs of the ultrafast demagnetization evidenced by Tengdin *et al.*[8]. This work is therefore in line with recent experimental work attributing the main part of the demagnetization as originating from transversal excitations[10–12].

Furthermore, as evidenced by the fact that the reduction of the inter-atomic exchange occurs by raising the electronic temperature in *ab initio* calculations, this mechanism does not rely on a direct light-matter interaction. This is in agreement with the experimental work of Bergeard *et al.*[39], showing that the presence of hot electrons is sufficient to induce an ultrafast demagnetization.

In conclusion, this work opens up new perspectives by considering the involvement of the light-induced inter-atomic exchange reduction in the demagnetization dynamics. While such a phenomenon has been widely overlooked, we find it to be directly correlated to the amplitude of the initial demagnetization. This provides an explanation of the paradoxically high demagnetization amplitude found in Ni, as compared to Co and Fe, which could not be rationalized otherwise.

-
- [1] E. Beaurepaire, J. C. Merle, A. Daunois, and J. Y. Bigot, *Physical Review Letters* **76**, 4250 (1996).
 - [2] C. D. Stanciu, F. Hansteen, A. V. Kimel, A. Kirilyuk, A. Tsukamoto, A. Itoh, and T. Rasing, *Physical Review Letters* **99**, 47601 (2007).
 - [3] I. Radu, K. Vahaplar, C. Stamm, T. Kachel, N. Pontius, H. A. Dürr, T. A. Ostler, J. Barker, R. F. Evans, R. W. Chantrell, A. Tsukamoto, A. Itoh, A. Kirilyuk, T. Rasing, and A. V. Kimel, *Nature* **472**, 205 (2011).
 - [4] S. Mangin, M. Gottwald, C. H. Lambert, D. Steil, V. Uhlř, L. Pang, M. Hehn, S. Alebrand, M. Cinchetti, G. Malinowski, Y. Fainman, M. Aeschlimann, and E. E. Fullerton, *Nature Materials* **13**, 286 (2014).
 - [5] C. H. Lambert, S. Mangin, B. S. S. Varaprasad, Y. K. Takahashi, M. Hehn, M. Cinchetti, G. Malinowski, K. Hono, Y. Fainman, M. Aeschlimann, and E. E. Fullerton, *Science* **345**, 1337 (2014).
 - [6] H. S. Rhie, H. A. Dürr, and W. Eberhardt, *Physical Review Letters* **90**, 4 (2003).
 - [7] M. Cinchetti, M. Sánchez Albaneda, D. Hoffmann, T. Roth, J. P. Wüstenberg, M. Krauß, O. Andreyev, H. C. Schneider, M. Bauer, and M. Aeschlimann, *Physical Review Letters* **97**, 177201 (2006), arXiv:0605272 [cond-mat].
 - [8] P. Tengdin, W. You, C. Chen, X. Shi, D. Zusin, Y. Zhang, C. Gentry, A. Blonsky, M. Keller, P. M. Oppeneer, H. C. Kapteyn, Z. Tao, and M. M. Murnane, *Science Advances* **4**, 1 (2018).
 - [9] W. You, P. Tengdin, C. Chen, X. Shi, D. Zusin, Y. Zhang, C. Gentry, A. Blonsky, M. Keller, P. M. Oppeneer, H. Kapteyn, Z. Tao, and M. Murnane, *Physical Review Letters* **121** (2018), 10.1103/PhysRevLett.121.077204.
 - [10] P. Scheid, Q. Remy, S. Lebègue, G. Malinowski, and S. Mangin, *Journal of Magnetism and Magnetic Materials* **560**, 169596 (2022).
 - [11] E. Turgut, D. Zusin, D. Legut, K. Carva, R. Knut, J. M. Shaw, C. Chen, Z. Tao, H. T. Nembach, T. J. Silva, S. Mathias, M. Aeschlimann, P. M. Oppeneer, H. C. Kapteyn, M. M. Murnane, and P. Grychtol, *Physical Review B* **94**, 220408(R) (2016).
 - [12] S. Eich, M. Plötzing, M. Rollinger, S. Emmerich, R. Adam, C. Chen, H. C. Kapteyn, M. M. Murnane, L. Plucinski, D. Steil, B. Stadtmüller, M. Cinchetti, M. Aeschlimann, C. M. Schneider, and S. Mathias, *Science Advances* **3**, 1 (2017).
 - [13] S. Jana, R. S. Malik, Y. O. Kvashnin, I. L. Locht, R. Knut, R. Stefanuik, I. Di Marco, A. N. Yaresko, M. Ahlberg, J. Åkerman, R. Chimata, M. Battiato, J. Söderström, O. Eriksson, and O. Karis, *Physical Review Research* **2**, 1 (2020), arXiv:1908.02872.
 - [14] K. Carva, M. Battiato, D. Legut, and P. M. Oppeneer, *Physical Review B - Condensed Matter and Materials Physics* **87**, 184425 (2013), arXiv:1305.3511.
 - [15] M. Battiato, K. Carva, and P. M. Oppeneer, *Physical Review Letters* **105**, 1 (2010), arXiv:1106.2117.
 - [16] P. Scheid, G. Malinowski, S. Mangin, and S. Lebègue, *Physical Review B* **99**, 174415 (2019).
 - [17] K. Krieger, J. K. Dewhurst, P. Elliott, S. Sharma, and E. K. Gross, *Journal of Chemical Theory and Computation* **11**, 4870 (2015).
 - [18] P. Scheid, G. Malinowski, S. Mangin, and S. Lebègue, *Physical Review B* **100**, 1 (2019).
 - [19] P. Scheid, S. Sharma, G. Malinowski, S. Mangin, and S. Lebègue, *Nano Letters* **21**, 1943 (2021).
 - [20] B. Koopmans, G. Malinowski, F. Dalla Longa, D. Steiauf, M. Fähnle, T. Roth, M. Cinchetti, and M. Aeschlimann, *Nature Materials* **9**, 259 (2010).
 - [21] T. Roth, A. J. Schellekens, S. Alebrand, O. Schmitt,

- D. Steil, B. Koopmans, M. Cinchetti, and M. Aeschlimann, *Physical Review X* **2** (2012), 10.1103/PhysRevX.2.021006.
- [22] D. Zahn, F. Jakobs, Y. W. Windsor, H. Seiler, T. Vasileiadis, T. A. Butcher, Y. Qi, D. Engel, U. Atxitia, J. Vorberger, and R. Ernstorfer, *Physical Review Research* **3**, 1 (2021), arXiv:2008.04611.
- [23] M. Pankratova, I. P. Miranda, D. Thonig, M. Pereiro, E. Sjöqvist, A. Delin, O. Eriksson, and A. Bergman, *Physical Review B* **106**, 1 (2022).
- [24] O. Gunnarsson, *Journal of Physics F: Metal Physics* **6**, 587 (1976).
- [25] J. R. Rumble, *CRC Handbook of Chemistry and Physics*, CRC Handbook of Chemistry and Physics (CRC Press, 2022).
- [26] U. Ritzmann, P. M. Oppeneer, and P. Maldonado, *Physical Review B* **102**, 214305 (2020), arXiv:1911.12414.
- [27] M. Haag, C. Illg, and M. Fähnle, *Physical Review B - Condensed Matter and Materials Physics* **90**, 14417 (2014).
- [28] M. C. Müller, S. Blügel, and C. Friedrich, *Physical Review B* **100**, 1 (2019), arXiv:1809.02395.
- [29] V. P. Antropov, M. I. Katsnelson, M. Van Schilfgaarde, and B. N. Harmon, *Physical Review Letters* **75**, 729 (1995).
- [30] V. Antropov, M. Katsnelson, B. Harmon, and M. van Schilfgaarde, *Physical Review B - Condensed Matter and Materials Physics* **54**, 1019 (1996).
- [31] S. Halilov, H. Eschrig, and A. Perlov, *Physical Review B - Condensed Matter and Materials Physics*, Tech. Rep. 1 (1998).
- [32] P. Kurz, F. Förster, L. Nordström, G. Bihlmayer, and S. Blügel, *Physical Review B - Condensed Matter and Materials Physics* **69**, 24415 (2004).
- [33] P. Hohenberg and W. Kohn, *Physical Review* **136**, B864 (1964).
- [34] W. Kohn and L. J. Sham, *Physical Review* **140**, A1133 (1965).
- [35] J. P. Perdew and Y. Wang, *Physical Review B* **45**, 13244 (1992).
- [36] J. Kudrnovský, I. Turek, M. Pajda, P. Bruno, and V. Drchal, *Physical Review B - Condensed Matter and Materials Physics* **64**, 174402 (2001), arXiv:0007441 [cond-mat].
- [37] E. Carpena, E. Mancini, C. Dallera, M. Brenna, E. Puppin, and S. De Silvestri, *Physical Review B - Condensed Matter and Materials Physics* **78** (2008), 10.1103/PhysRevB.78.174422.
- [38] D. A. Garanin, *Phys. Rev. B* **53**, 11593 (1996).
- [39] N. Bergeard, M. Hehn, S. Mangin, G. Lengaigne, F. Montaigne, M. L. Lalieu, B. Koopmans, and G. Malinowski, *Physical Review Letters* **117** (2016), 10.1103/PhysRevLett.117.147203.